Electrochimica Acta 303 (2019) 204–210

Contents lists available at ScienceDirect

Electrochimica Acta

journal homepage: www.elsevier.com/locate/electacta

Effects of carbon dots on ZnO nanoparticle-based dye-sensitized solar cells

Mulugeta Tesema Efa [a], Toyoko Imae [a, b, *]

[a] Graduate Institute of Applied Science and Technology, National Taiwan University of Science and Technology, Taipei, 10607, Taiwan
[b] Department of Chemical Engineering, National Taiwan University of Science and Technology, Taipei, 10607, Taiwan

ARTICLE INFO

Article history:
Received 10 August 2018
Received in revised form
31 January 2019
Accepted 3 February 2019
Available online 4 February 2019

Keywords:
Carbon dot
Zinc oxide nanoparticle
Dye-sensitized solar cell
Photovoltaic measurement
Photovoltaic conversion efficiency

ABSTRACT

ZnO nanoparticles have been assessed the effects of added carbon dots (Cdots) on the performance of photovoltaic devices: ZnO(100) and ZnO(20) with particle sizes of 94 and 20 nm, respectively, were hybridized with Cdots and characterized by current–voltage measurements under the illumination condition. The photovoltaic conversion of dye-sensitized solar cells (DSSCs) was effective for ZnO(20) superior to Zn (100) and for the incorporation of 10 wt% Cdots in the hybrid nanostructures. Moreover, when the mole ratio (ethylenediamine:citric acid) between raw materials of Cdots was 2:1, the conversion efficiency was highest (5.9%), and this value was 7 times higher than that of ZnO(20) DSSC without Cdots. Electrochemical impedance spectroscopy also showed that the charge transfer resistance property was lowest for Cdots(2:1)-hybridized ZnO(20) DSSC. It can be thus concluded that the performance of ZnO-based DSSCs is improved by the size-minimization of ZnO and the addition of adequate amount of Cdots. The effect of carbon dots was discussed based on electron transfer between ZnO and Cdots under the illumination.

1. Introduction

The semiconducting materials have been taken notice due to their valuable applications in light harvesting systems such as solar energy conversion, photovoltaic and photocatalytic devices, since they have nonlinear properties because of their distorted electronic properties [1,2]. However, since an inorganic semiconductor with a wide band gap at room temperature is disadvantageous for visible light harvesting, semiconductors with a narrow band gap like quantum dots [3] or composites of inorganic semiconducting materials with other metal nanoparticles are usable raising the efficiency of visible light harvesting [4].

Nanocomposites are effective, multifunctional materials for energy conversion or photochemical reaction and in electrochemical supercapacitors. They enhance the photocatalytic performance by improving their electronic and structural properties. Currently, nanocomposites of ZnO with carbon-based materials like graphene and carbon nanotubes were fabricated by employing various methods for achieving high performance for supercapacitor and energy conversion [5–7]. However, these electrodes showed to have limited improvements in the light harvesting performance [6]. Hence, the electrodes must be developed to modify to display the better performance.

Carbon dots (Cdots) are one of carbon materials as well as carbon nanotubes but they are highly ecofriendly materials due to the cheap cost of raw materials and the possible production from waste materials, different from carbon nanotube [8]. Moreover, their composites with conducting polymers exerted the strong performance on the pseudo-capacitor, that is, the composite electrodes of polypyrrole@Cdots or polyaniline@Cdots enhanced more than double of the specific capacitances of pristine conducting polymers by their synergetic effect [9]. In our previous publication, we hybridized Cdots with ZnO nanoparticles and it has been found that the optical band gap of ZnO significantly reduced with addition of Cdots [10]. This indicates the possible performance of ZnO/@Cdots composites on photocatalysis [8] and photovoltaic electrochemistry. Thus, the performance of ZnO-based photoreaction devices may be enhanced by additives which have an effect on the band gap of ZnO [11,12], and Cdots possess possibilities to improve the performance of ZnO-based photovoltaic electrochemistry by their adsorption on ZnO.

In this work, based on the above concept, the exploration of electrochemical performance by nanocomposite materials of ZnO

* Corresponding author. Graduate Institute of Applied Science and Technology, National Taiwan University of Science and Technology, Taipei, 10607, Taiwan.
E-mail address: imae@mail.ntust.edu.tw (T. Imae).

https://doi.org/10.1016/j.electacta.2019.02.012
0013-4686/

with Cdots were performed for energy conversion, especially, on dye-sensitized solar cells (DSSCs). DSSCs were constructed by ZnO nanoparticles with different particle sizes as the semiconductor using rhodamine B (RhB) and *cis*-diisothiocyanato-bis(2,2-bipyridyl-4,4-dicarboxylato) ruthenium (II) bis(tetrabutylammonium) (N-719) dyes as a principal sensitizer and energy acceptor. The effects of Cdots were examined at the different amounts of added Cdots, and the nitrogen content in Cdots was varied by changing the ratio of raw materials (ethylenediamine and citric acid). Thus, the Cdots are expected to be the promising additive for enhancing photovoltaic performance.

2. Experimental section

Ethylenediamine (99%), citric acid anhydrous (99%), and RhB were purchased from Acros organics (USA). N719 was purchased from SORALONIX (Germany). ZnO nanoparticles (ZnO(100) and ZnO(20) with particle sizes of 94 and 20 nm, respectively) were same samples previously synthesized and characterized [10]. They were prepared using calcination and polyol solvent synthesis methods [10,13], respectively, and characterized using the transmission electron microscopy, X-ray diffraction, X-ray photoelectron spectroscopy, infrared absorption spectroscopy, nitrogen adsorption-desorption isotherm analysis and band gap determination [10].

Cdots with different nitrogen contents were synthesized via a method that described in the previous work [10]. Citric acid anhydrous (1 g) was dissolved in water (70 ml) and adequate amount of ethylenediamine (0.30–1.05 ml) was added to be the mole ratios of ethylenediamine against citric acid of 1:1, 1.5:1, 2:1, 2.5:1, 3:1 and 3.5:1, which were hereafter described Cdots(x = 1, 1.5, 2, 2.5, 3, 3.5). After the mixture was stirred for 30 min at room temperature, it was hydrothermally carbonized in an autoclave for 5 h at 250 °C and stood to cool. The solvent was evaporated and the resulted Cdots were dried for 3 h at 100 °C. ZnO (400 mg) in isopropanol (2 ml) and Cdots (48 mg, 10 wt%) in water (2 ml) were mixed, sonicated for 10 min and stirred for 4 h at room temperature. ZnO@Cdots were filtered, washed several times with water, air-dried overnight and heat-dried at 100 °C for 3 h. The concentration of Cdots (10 wt%) was maintained in whole experiments except the concentration dependence examination of Cdots.

Electrochemical measurements were carried out using a Zahner CIMPS-X Photo-Electrochemical Workstation together with the THALES software package (Xpot-26366) on a photovoltaic cell of a two-electrode configuration with a ZnO@Cdots working electrode and a Pt counter electrode, which were prepared by following procedure: ZnO@Cdots paste (mixture of ZnO@Cdots (100 mg) with isopropanol (0.5 ml)) was spin-coated on an indium tin oxide (ITO) glass substrate and dried for 30 min at 400 °C. The temperature was varied at 25–450 °C for the temperature dependence examination of dye adsorption. The ZnO@Cdots-coated electrode was immersed into an ethanolic dye solution (0.5 mM) for 5 h at room temperature and rinsed with ethanol. The determination of adsorbed dye amount on ZnO@Cdots/dye electrode was performed by desorbing dye for 12 h in a 0.1 M NaOH solution of a mixed solvent of water and ethanol (by volume ratio 1:1) and evaluating by means of spectrocolorimetry at 540 and 500 nm absorption bands of RhB and N719, respectively. The counter electrode was prepared by sputter deposition of Pt (9 nm thickness) onto the ITO glass substrate (at 20 mA sputtering current and 90 s sputtering time on a Cressingion 108 auto coater). To assemble the solar cells, a Pt-coated ITO glass was placed on the dye-adsorbed ZnO@Cdots-coated photoelectrode spaced by a 0.13 mm paraffin spacer, and a small quantity of a redox electrolyte solution (an acetonitrile solution of KI (0.3 M) and I_2 (0.05 M) was injected between two electrodes through the small hole created on the Pt counter electrode [8]. From the measurements of current-voltage (I-V) characteristics, the conversion efficiency η was calculated based on an equation of $\eta = Jsc \cdot Voc \cdot FF/Iph$, where *J*sc is the short-circuit current density, *V*oc is the open-circuit voltage, FF is the fill factor, and *I*ph is the source of stimulated light at 156 w/m^2. The electrochemical impedance spectroscopic (EIS) measurements were carried out using an impedance-measuring mode on the same instrument. It was recorded at a frequency range of 10 kHz–10 Hz using a solar simulator. The fluorescence spectra were recorded on a HITACHI photoluminescence spectrophotometer. The solution cell thickness was 10 mm.

3. Results and discussion

3.1. Electrochemical characterization

Photovoltaic testing, that is, I-V characterization of DSSCs can be progressed by a narrow band-monochromated light source. Furthermore, a meaningful effect on the performance of the DSSCs may occur from the chemical structure of dyes for sensitization and depend on adsorbed time/amounts of dyes on ZnO surface [14]. To investigate the wavelength dependence of incident visible light on the photoexcitation behavior of dyes, three different light sources, namely, blue (430 nm), green (523 nm), and red (630 nm) light emitting diode (LED) lights at the same light intensity (56 w/m^2) were applied for ZnO nanoparticle-based DSSCs with RhB and N719 dyes, since light source and dye species depend on photovoltaic [15]. Electrochemical measurements were carried out on a two-electrode configuration with ITO/ZnO@Cdots as a working-electrode and Pt electrode as a counter-electrode. Fig. 1 shows the I-V characteristics of ZnO@Cdots nanoparticle-based DSSCs. With increasing wavelength of light sources from blue to red, the I-V characteristics decreased for both RhB- and N719-sensitized DSSCs. Thus, only blue light source was hence forth utilized on whole experiments

Thus, experimental comparisons among composite DSSCs consisting of ZnO@Cdots/dye nanostructures were performed at different Cdots contents and ethylenediamine/citric acid mole ratio under blue light source at illumination intensity of 156 w/m^2. Fig. 2 shows I-V characteristics of different combinations of DSSCs regarding ZnO@Cdots (1) and sensitizers at various Cdots contents of 0–50 wt%. I-V curves were commonly intensified from 0 wt% up to 10 wt% Cdots content but weakened above this content. It was highest for N719-photosensitized ZnO(20)@Cdots DSSC. Moreover, the current from ZnO(20)@Cdots DSSC was 1.2–1.5 times higher than that from ZnO(100)@Cdots DSSC, and both ZnO(100)@Cdots and ZnO(20)@Cdots DSSCs were intensified their current (about one order) and voltage (1.3–2.0 times), when sensitizer was varied from RhB to N719. These insights indicate the more predominant efficiency of small ZnO than large ZnO and of N719 than RhB. Fig. 3 displays I-V curves from ZnO@Cdots/dye DSSCs at different ethylenediamine/citric acid mole ratios of 1.5–3.5. For the case of different ethylenediamine/citric acid mole ratio, photovoltaic and device performances were improved at ethylenediamine/citric acid mole ratio of 2 and more dominant for N719 than RhB and for ZnO(20)@Cdots than ZnO(100)@Cdots.

The electrical properties of DSSCs, namely, short circuit current density (Jsc), open circuit voltage (V_{oc}), fill factor (FF) and conversion efficiency (η) can be evaluated from I–V characteristics and they were plotted as a function of Cdots content and ethylenediamine/citric acid mole ratio as shown in Fig. 4 and listed in Table 1. As seen in Fig. 4A, open circuit voltage slightly depended on size of ZnO, sensitizer species and Cdots content but still within a range of minimum 0.20 V and maximum 0.57 V, and fill factor was most

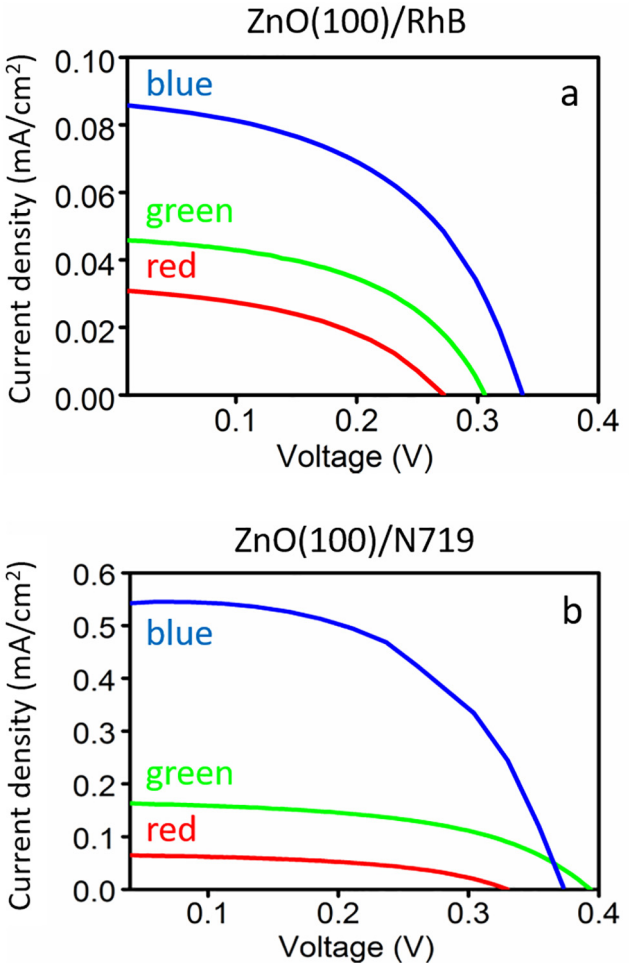

Fig. 1. Light source dependency on I–V characteristics of (a) ZnO(100)/RhB and (b) ZnO(100)//N719 under blue, green and red light sources at illumination intensity of 56 w/m^2.

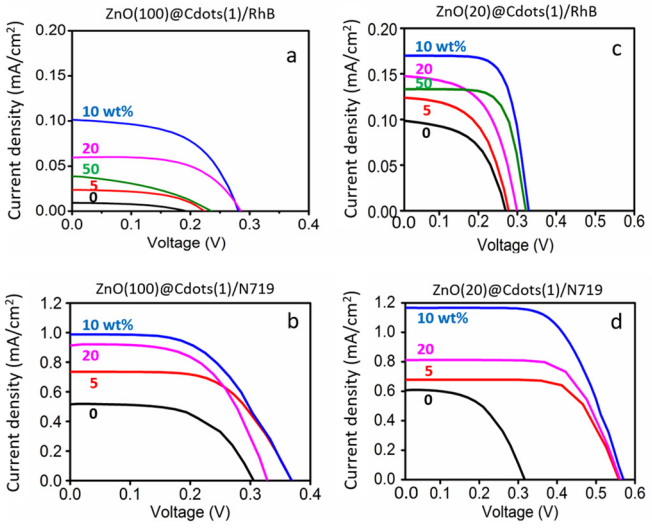

Fig. 2. Cdots content dependency on I-V characteristics of ZnO@Cdots/dye DSSCs. (a) ZnO(100)@Cdots(1)/RhB, (b) ZnO(100)@Cdots(1)/N719, (c) ZnO(20)@Cdots(1)/RhB and (d) ZnO(20)@Cdots(1)/N719. Cdots content: 0, 5, 10, 20 and 50 wt%.

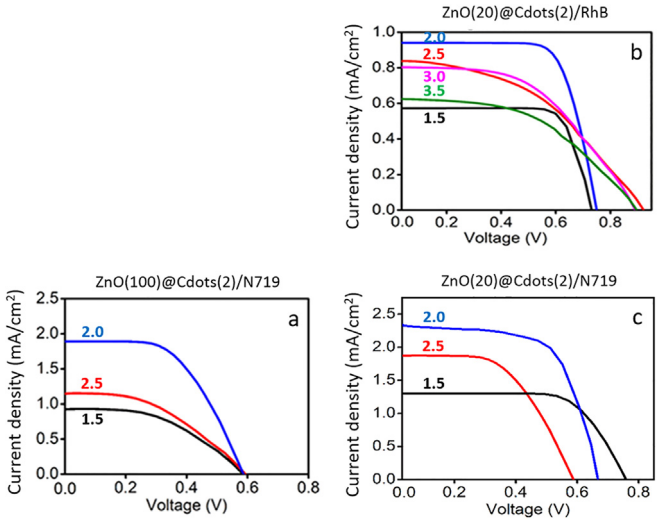

Fig. 3. Ethylenediamine/citric acid mole ratio dependency on I–V characteristics of ZnO@Cdots/dye DSSCs. (a) ZnO(100)@Cdots(2)/N719, (b) ZnO(20)@Cdots(2)/RhB and (c) ZnO(20)@Cdots(2)/N719. Ethylenediamine/citric acid mole ratio: 1.5, 2, 2.5, 3 and 3.5.

independent of the variation of such factors. However, short circuit current density and accordingly conversion efficiency remarkably depended on such factors: They were always maximum at 10 wt% Cdots content, numerical values from N719-sensitized cells were almost one order higher than those from RhB-sensitized cells, and numerical values of conversion efficiency from ZnO(20)@Cdots(1) were almost double from ZnO(100)@Cdots(1) DSSCs. Thus, the effective composite DSSC was of ZnO(20)@Cdots(1)/N719 nanostructures at 10 wt% Cdots content.

The electrochemical properties of DSSCs depending on ethylenediamine/citric acid mole ratio were evaluated for ZnO(20)@Cdots/RhB, ZnO(100)@Cdots/N719 and ZnO(20)@Cdots/N719 and plotted in Fig. 4B. Open circuit voltage and fill factor did not so much depend on ethylenediamine/citric acid mole ratio and displayed similar values for three DSSCs. However, short circuit current density and, thus, conversion efficiency were meaningfully influenced on ethylenediamine/citric acid mole ratio at the order of ZnO(20)@Cdots/RhB < ZnO(100)@Cdots/N719 < ZnO(20)@Cdots/N719, and the parameters were commonly highest at 2:1 ethylenediamine:citric acid mole ratio, that is, at ZnO(20)@Cdots(2). Finally, the highest conversion efficiency (5.9%) was attained by ZnO(20)@Cdots(2)/N719 DSSC.

3.2. Efficiencies of size of ZnO and addition of cdots on DSSC performance

The efficiency of size of ZnO on performance of DSSCs, that is, the more superior efficiency by ZnO(20) than by ZnO(100) can be explained by the increased surface area per volume provided by the nanostructures, as demonstrated in the previous report [10]. The large surface area is effective for promoting the adsorption of sensitizer molecules, the photoenergy absorption by sensitizer molecules and the stimulation of photovoltaic effect by semiconductive materials. Regarding sensitizer molecules, N719 could be more effective than RhB. Moreover, the addition of Cdots on the photoelectrode improved the conversion efficiency. This result is relating to the fact that the addition of Cdots increased the surface area of ZnO@Cdots nanoparticles, as reported in the previous paper

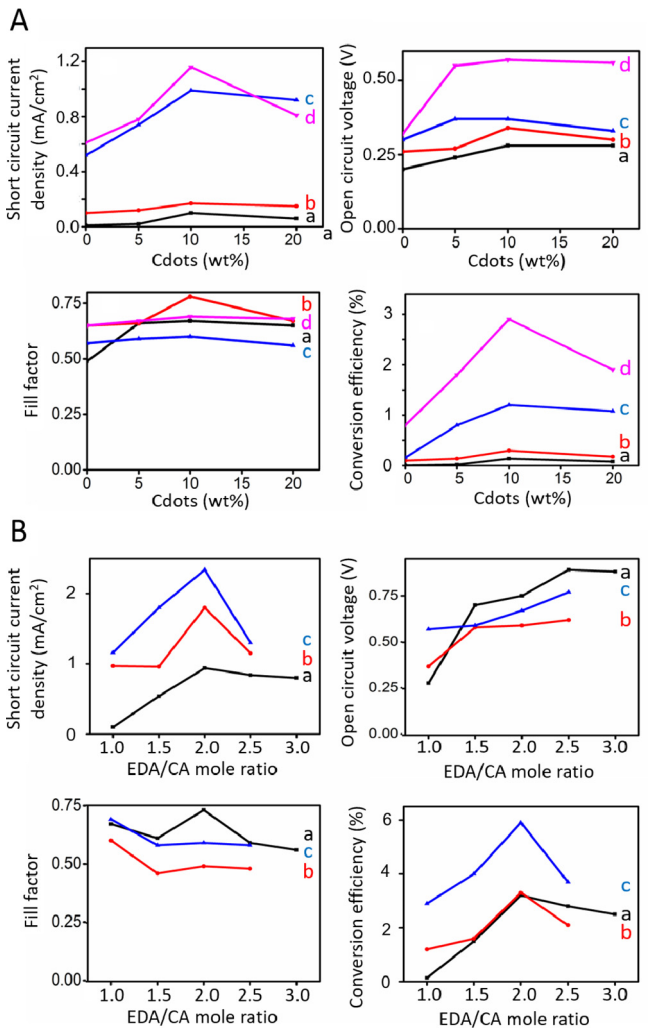

Fig. 4. Plots of electrochemical parameters from ZnO@Cdots/dye DSSCs. (A) As a function of Cdots content for (a) ZnO(100)@Cdots(1)/RhB, (b) ZnO(20)@Cdots(1)/RhB, (c) ZnO(100)@Cdots(1)/N719 and (d) ZnO(20)@Cdots(1)/N719. (B) As a function of ethylenediamine/citric acid (EDA/CA) mole ratio for (a) ZnO(20)@Cdots/RhB, (b) ZnO(100)@Cdots/N719 and (c) ZnO(20)@Cdots(1)/N719.

[10]. In addition, the highest current density was attained at the limited Cdots amount (in the present case, at 10 wt% Cdots), but the further addition of Cdots decreased the activities of ZnO@Cdots. The changes of the NH_2 content in Cdots could also provide the strong influence on the DSSC performance, indicating the significant effect of nitrogen on photocurrent density. The increase of conversion efficiency from 2.9% at 1:1 ethylenediamine:citric acid mole ratio to 5.9% at 2:1 ethylenediamine:citric acid mole ratio on ZnO(20)@Cdots/N719 DSSCs is remarkable.

To discuss the results described above, dye adsorption, EIS and photoluminescence were additionally examined. The adsorbed amount of RhB and N719 dyes on ZnO@Cdots/dye electrodes was determined by calorimetrically analyzing [16]. As indicated in Table 2, the absorbed amount of both dyes increased with increasing the pre-heating temperature (before dye adsorption) of ZnO(20)@Cdots(2) from 25 °C up to 400 °C and then decreased at higher temperature (450 °C). By heating, the organic materials are calcined and inorganic particles are expected to have larger surface area, which is more convenient for dye adsorbing. The adsorption of N719 dye was larger than that of RhB, and this result is consistent with the DSSC performance, indicating the relation of dye adsorption and DSSC performance. The direct relation between them are obvious from numerical values listed in Table 2, which were calculated from I-V characteristics (Fig. 5) of ZnO(20)@Cdots(2)/N719 DSSCs prepared at different temperatures: The conversion efficiency was highest for a DSSC treated a 400 °C. Namely, the increase in adsorption of dye can result in a better light harvesting and high-power conversion efficiency [16]. By the way, the adsorption of N719 was 3–5 times higher on ZnO(20)@Cdots(2) than on ZnO(100)@Cdots(2) (Table 2). It can be referred that the efficiency of solar cell device strongly relates to the large amount of adsorption of sensitizer molecule on small ZnO nanoparticles with large surface area [10].

EIS measurement was performed for ZnO(20), ZnO(20)@Cdots(1) and ZnO(20)@Cdots(2) electrodes. As seen in Fig. 6, the diameter of the Nyquist semicircle lessened in the order of ZnO(20) > ZnO(20)@Cdots(1) > ZnO@Cdots(2), indicating that the resistance weakened in this order [9]. The ohmic series resistance Rs and the charge transfer resistance Rct were obtained based on Randles equivalent circuit model and listed in Table 3. Both resistances decreased after the addition of Cdots, and the increase in nitrogen content in Cdots also decreased both resistance values. Table 3 includes the conversion efficiency evaluated from I-V characteristics of corresponding DSSCs (Figs. 2 and 3). The conversion efficiency increased with the decrease of resistances, which directly prove the roles of Cdots and nitrogen associated with the conversion efficiency and the charge-transfer in the solar cells. Namely, the addition of Cdots with abundant nitrogen content facilitates the split to photoinduced electron–hole pairs in ZnO and the transfer of the electron to the ITO to gain the preferable photo conversion efficiency.

ZnO has been widely used for the solar energy conversion. However, the applicability of ZnO in visible light is limited because of the wide band gap of the material, which results in low efficiency during solar photo conversion. Our previous result showed that the incorporation of carbon decreases the energy bandgap of ZnO [10], and this phenomenon should improve the separation efficiency to electron-hole pairs, and significantly enhance the visible light photocatalytic activity. In addition, the photoluminescence (PL) spectra of ZnO and its composite materials with dye may be related to the generation and transfer of the photo-induced electrons. Fig. 7 shows the PL spectra of ZnO(20), ZnO(20)@Cdots(2) and Cdots(2), and Table 4 lists their PL bands. ZnO(20) had two excitation bands at 265 and 378 nm and their corresponding emission band at 335 and 440 nm, respectively, although PL bands at high excitation wavelength had stronger intensity than those at low excitation wavelength. Two excitation bands of Cdots(2) were at 245 and 350 nm and the corresponding emission bands were at 440 and 448 nm, respectively. PL bands at both excitation wavelengths had similar intensity and the intensities were more than one order larger than those of ZnO(20).

Then ZnO(20)@Cdots(2) possessed three excitation bands due to the contributions from both ZnO(20) and Cdots(2), and emission bands correspondingly varied, although the intensities of PL bands were similar to those of ZnO(20) but smaller than those of Cdots. Yamada et al. [17] have estimated, by the computer simulation, the principle for the efficient increase of solar electric generation that the dissipation of energy subserves the conversion of light to electric current. Cammi et al. [18] have concluded that the increase of device photoresponse is attributed to the fast injection of photoexcited electron from the Cdots into the conduction band of ZnO, although they did not directly refer about the decrease of PL. Thus, the contribution of carbon dots on the solar cell for the efficient increase of solar electric generation can be considered in view of the result of PL and the reports in literature. That is, the photo-energy absorbed by Cdots is transferred to ZnO, ZnO loses it by the

Table 1
Electrical properties of DSSCs evaluated from I-V characteristics.

Photo anode	Cdots (wt%)	Ethylenediamine:citric acid	J_{SC} (mA/cm^2)	V_{oc} (V)	FF	η (%)
ZnO (100)/RhB	0	1:1	0.01 ± 0.001	0.20 ± 0.10	0.49 ± 0.02	0.005 ± 0.002
	5	1:1	0.02 ± 0.001	0.24 ± 0.12	0.66 ± 0.22	0.02 ± 0.003
	10	1:1	0.10 ± 0.04	0.28 ± 0.10	0.67 ± 0.01	0.14 ± 0.08
	20	1:1	0.06 ± 0.01	0.28 ± 0.07	0.65 ± 0.04	0.08 ± 0.02
	50	1:1	0.04 ± 0.02	0.25 ± 0.01	0.55 ± 0.02	0.03 ± 0.002
ZnO (20)/RhB	0	1:1	0.10 ± 0.01	0.26 ± 0.01	0.65 ± 0.02	0.10 ± 0.04
	5	1:1	0.12 ± 0.01	0.27 ± 0.01	0.66 ± 0.20	0.14 ± 0.03
	10	1:1	0.17 ± 0.01	0.34 ± 0.02	0.78 ± 0.02	0.30 ± 0.03
	20	1:1	0.15 ± 0.02	0.30 ± 0.02	0.67 ± 0.03	0.18 ± 0.04
	50	1:1	0.13 ± 0.03	0.31 ± 0.01	0.60 ± 0.01	0.16 ± 0.02
ZnO (100)/N719	0	1:1	0.52 ± 0.10	0.30 ± 0.01	0.57 ± 0.10	0.16 ± 0.02
	5	1:1	0.74 ± 0.03	0.37 ± 0.02	0.59 ± 0.20	0.80 ± 0.01
	10	1:1	0.99 ± 0.10	0.37 ± 0.02	0.60 ± 0.30	1.20 ± 0.30
	20	1:1	0.92 ± 0.02	0.33 ± 0.10	0.56 ± 0.05	1.08 ± 0.10
ZnO (20)/N719	0	1:1	0.61 ± 0.10	0.32 ± 0.02	0.65 ± 0.01	0.80 ± 0.01
	5	1:1	0.78 ± 0.20	0.55 ± 0.10	0.67 ± 0.02	1.80 ± 0.30
	10	1:1	1.16 ± 0.03	0.57 ± 0.05	0.69 ± 0.01	2.90 ± 0.10
	20	1:1	0.81 ± 0.02	0.56 ± 0.01	0.68 ± 0.03	1.90 ± 0.05
ZnO(20)@Cdot	10	1.5:1	0.54 ± 0.04	0.70 ± 0.05	0.61 ± 0.01	1.52 ± 0.01
/RhB	10	2.0:1	0.94 ± 0.02	0.75 ± 0.02	0.73 ± 0.10	3.24 ± 0.30
	10	2.5:1	0.84 ± 0.01	0.89 ± 0.03	0.59 ± 0.10	2.81 ± 0.05
	10	3.0:1	0.80 ± 0.04	0.88 ± 0.02	0.56 ± 0.30	2.50 ± 0.10
	10	3.5:1	0.62 ± 0.02	0.88 ± 0.03	0.42 ± 0.01	1.44 ± 0.02
ZnO(100)@Cdot	10	1.5:1	0.95 + 0.05	0.58 ± 0.02	0.46 ± 0.10	1.63 ± 0.02
/N719	10	2.0:1	1.80 ± 0.01	0.59 ± 0.02	0.49 ± 0.01	3.33 ± 0.40
	10	2.5:1	1.15 ± 0.03	0.62 ± 0.10	0.48 ± 0.03	2.16 ± 0.05
ZnO(20)@Cdot	10	1.5:1	1.80 ± 0.01	0.59 ± 0.02	0.58 ± 0.04	4.00 ± 0.20
/N719	10	2.0:1	2.34 ± 0.03	0.67 ± 0.10	0.59 ± 0.05	5.92 ± 0.01
	10	2.5:1	1.30 ± 0.04	0.77 ± 0.03	0.58 ± 0.30	3.74 ± 0.04

Table 2
Adsorption amounts of RhB and N719 on ZnO@Cdots electrodes treated at different temperatures and a photovoltaic parameter from ZnO(20)@Cdots(2)/N719 electrode.

Temperature (^{0}C)	Adsorption amount (mg/mg(electrode))			η (%)
	ZnO(20)@Cdot(2)/RhB	ZnO(100)@Cdot(2)/N719	ZnO(20)@Cdot(2)/N719	ZnO(20)@Cdot(2)/N719
25	0.018	–	0.06	1.6
200	0.024	–	0.09	2.8
350	0.032	0.04	0.14	5.7
400	0.043	0.07	0.25	5.9
450	0.028	0.056	0.11	5.5

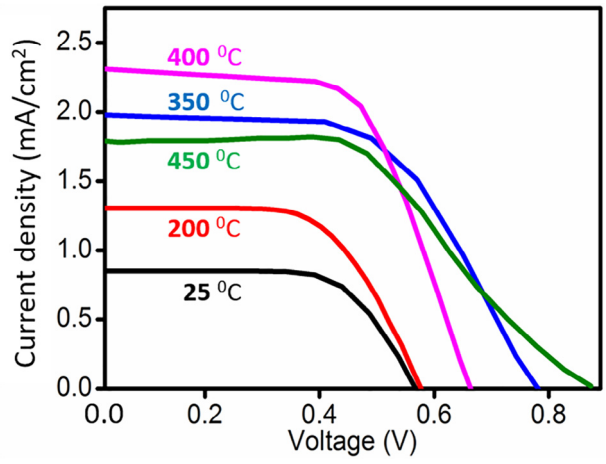

Fig. 5. I–V characteristics for ZnO(20)@Cdots(2)/N719 DSSCs at pre-heated temperatures of 25, 200, 350, 400 and 450 °C.

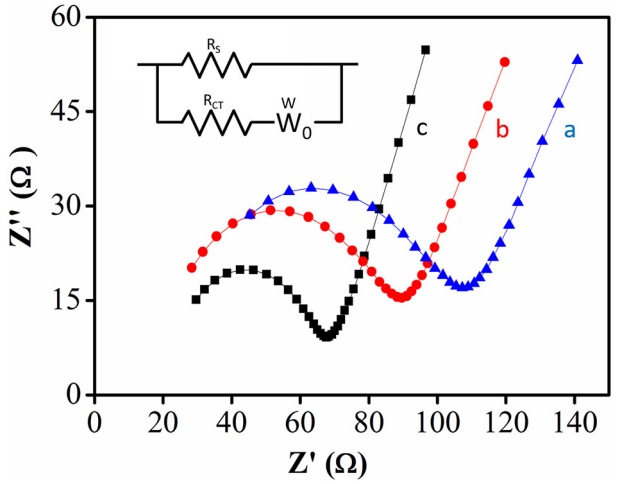

Fig. 6. Nyquist plots of (a) ZnO(20), (b) ZnO(20)@Cdots(1) and (c) ZnO(20)@Cdots(2). Inset indicates Randles equivalent circuit.

dissipation, and the excess dissipation promotes the electron-hole separation for raising the additional electric current. as one of possible contribution of Cdots. It should be noted that a preferable electron accumulation by the suppression of electron-hole recombination may also be caused by Cdots in the Cdots-adsorbed ZnO particle and contribute to the enhancement of the current density. Cdots also will behave as a donor to supply electron

Table 3
Parameters from EIS and I-V curves for ZnO(20) and ZnO(20)@Cdots DSSCs.

cell	Rs (Ω)	Rct (Ω)	η (%)
ZnO(20)	45.3	72.8	0.8
ZnO(20)@Cdots(1)	29.4	69.6	2.9
ZnO(20)@Cdots(2)	28.4	40.3	5.9

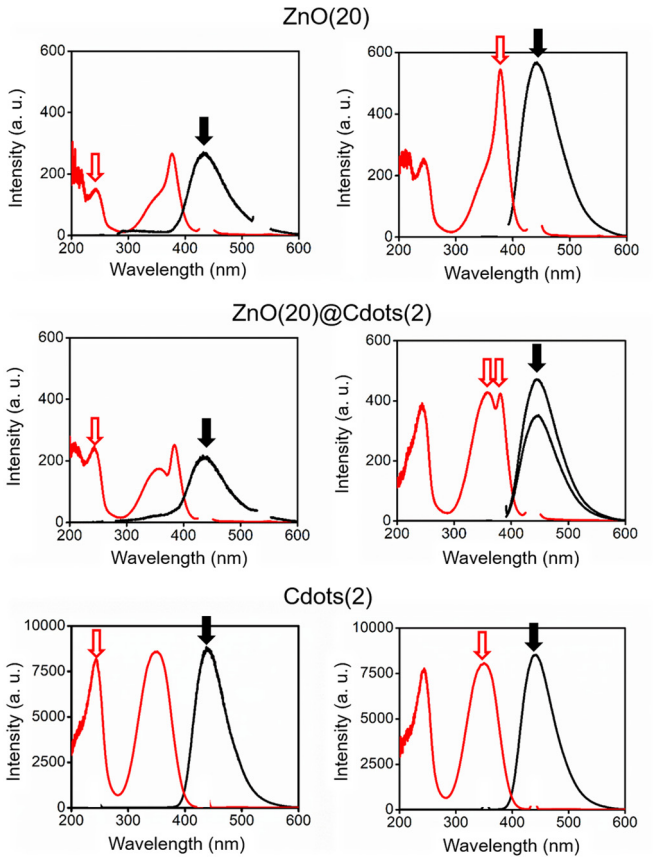

Fig. 7. Excitation and emission PL spectra of ZnO(20), ZnO(20)@Cdots(2) and Cdots. Open arrow indicates an excitation wavelength for measuring emission spectrum and closed arrow indicates an emission wavelength for measuring excitation spectrum.

to n-type semiconductor, which gives rise to the decrease of band gap.

Thus, the addition of Cdots subserved the conversion of light to electric current but its efficiency was maximized at 10 wt% Cdots (see Fig. 4). The further addition of Cdots decreases the activity of electron-hole separation in ZnO due to the decrease of dye molecules directly adsorbed on ZnO because of the excess direct adsorption of Cdots on ZnO surface. Incidentally, the adsorption of N719, which was measured by calorimetry, was 0.25, 0.08, and 0.033 mg/mg(electrode) for 10, 20 and 50 wt% Cdots, respectively. The photovoltaic performance is enhanced by increasing the ethylenediamine/citric acid mole ratio in Cdots, because the PL of Cdots is intensified with increasing ethylenediamine/citric acid mole ratio. Thus, the contribution of Cdots by thermal dissipation raises.

Scheme 1 illustrates the schematic anode in the present work. The device is constructed by ZnO, Cdot, dye and ITO. The dye sensitizer is excited by the emitted visible light, and the excited photoenergy induces the electron-hole separation in ZnO. Separately, Cdots also contribute to enhance the photovoltaic effect of ZnO by the electron transfer from Cdot donor to the conductive band level of n-type semiconductor ZnO, by the suppression of electron-hole recombination in ZnO or by the donation of the energy in Cdots excited by visible light. The separated electrons are transferred to ITO substrate. Then the amine in Cdot as electron donor also encourages the donation of energy.

As ZnO DSSC produces low conversion efficiency as seen in Table 1, ZnO-based DSSC researches have been relating to the dependence to crystal structures of ZnO and the effect of additives [19,20]. On the other hand, the present investigation confirmed the role of particle size on DSSC, as smaller size is generable the larger

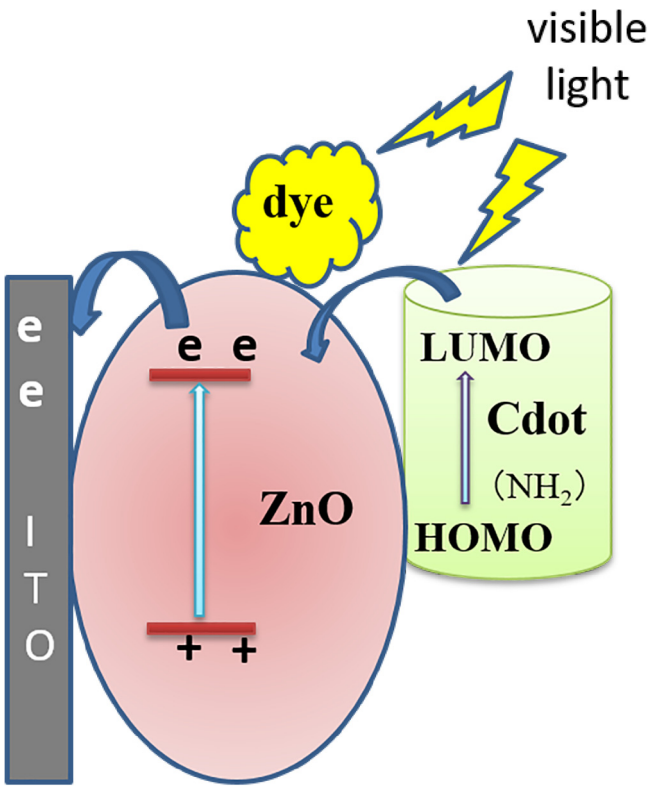

Scheme 1. Schematic illustration of anode in DSSC.

Table 4
PL bands of ZnO(20), ZnO(20)@Cdots(2) and Cdots(2).

phosphor	λ_{ex} (nm)	Excitation intensity (a.u.)	λ_{em} (nm)	Emission intensity (a.u.)
ZnO(20)	265	150	435	250
	378	543	440	567
ZnO(20)@Cdot(2)	265	220	435	200
	366	430	440	352
	380	425	440	474
Cdots(2)	245	7790	440	8805
	350	8070	448	8575

surface area for the adsorption of photosensitizer and the resultant higher conversion efficiency. Incidentally, reports on enhancing the performance of ZnO-based DSSCs by adding carbon-based nanostructures are scarce. ZnO DSSC was enhanced the conversion efficiency to be 0.684% after it was incorporated single-walled carbon nanotubes [21]. ZnO-reduced graphene oxide nanocomposite has been employed as the photoanode in a DSSC, and the cell showed a photo conversion efficiency of 3.19 [22]. Spattered graphene on ZnO produced the efficiency of 3.98% [23].

The merit of Cdots is eco-friendly, low cost and easy preparation different from graphene, graphene oxide and carbon nanotubes and, most recently, Cdots-incorporated DSSCs have been reported. Carbon quantum dots were prepared from different carbon sources through a hydrothermal route, and bee-pollen-based carbon quantum dots on a TiO_2 anode achieved the power conversion efficiency of 0.11% [24]. Although carbon quantum dots were grown onto TiO_2 surfaces in situ, a power conversion efficiency was of 0.87% [25]. When nanostructured polyaniline was prepared using surface-passivated carbon dots by poly(ethylene imine) as a dopant and nucleating agent, this composite showed a maximum power conversion efficiency of 3.65% on photovoltaic study [26]. Carbon quantum dot-tailored CoSe was used as counter electrode in a DSSC device of a mesoscopic dye–TiO_2 photoanode and an I^-/I_3^- redox electrolyte, and this device yielded the efficiency of 7.01% [27]. The present work used Cdots-ZnO composites presented the larger or comparable conversion efficiency in comparison with the previous reports.

4. Conclusions

In this work, investigations to improve the performance of DSSCs consisting of two sizes of ZnO by the addition of Cdots were reported. ZnO of small size (20 nm) possessed large surface area per volume and thus ZnO(20) presented higher adsorption ability of sensitizer and higher performance than ZnO(100). Small particle size is also favorable for quick attainment of photoexcited electron-hole pair separation in conducting nanoparticles. This phenomenon affected on the increase of short current density and thus conversion efficiency. Meanwhile, the addition of Cdots to ZnO also enhanced the photovoltaic performance. The potency of Cdots is the contribution to the electron-hole pair separation in conducting nanoparticles in the different ways from photosensitizer, although the maximum performance of Cdots was at the confined content (10 wt%), since the excess adsorption of Cdots reduced the performance of photosensitizer because of the reduction of its adsorption on ZnO. The present investigation confirmed that the conversion efficiency of DSSC fabricated with ZnO@Cdots/N719 was 5.9% at 2:1 mol ratio of ethylenediamine/citric acid in Cdots. This investigation demonstrated the performance on DSSCs by adding low-cost additives but high-effective contribution (Cdots).

Acknowledgements

This investigation was partly supported by Ministry of Science and Technology, Taiwan (MOST 106-2221-E-011-121-). MTE gratefully acknowledges the financial support from National Taiwan University of Science and Technology, Taiwan, by a student scholarship.

References

[1] N.K. Elumalai, C. Vijila, R. Jose, A. Uddin, S. Ramakrishna, Metal oxide semiconducting interfacial layers for photovoltaic and photocatalytic applications, Mater Renew Sustain Energy 4 (2015) 11, https://doi.org/10.1007/s40243-015-0054-9.
[2] M. Ye, X. Wen, M. Wang, J. Iocozzia, N. Zhang, C. Lin, Z. Lin, Recent advances in dye-sensitized solar cells: from photoanodes, sensitizers and electrolytes to counter electrodes, Mater. Today 18 (2015) 155–162.
[3] Y. Li, Y. Hu, Y. Zhao, G. Shi, L. Deng, Y. Hou, L. Qu, An electrochemical avenue to green-luminescent graphene quantum dots as potential electron-acceptors for photovoltaics, Adv. Mater. 23 (2011) 776–780.
[4] M.A. Johar, R.A. Afza, A.A. Alazba, U. Manzoor, Photocatalysis and bandgap engineering using ZnO nanocomposites, Ann. Mater. Sci. Eng. 2015 (2015). https://doi.org/10.1155/2015/934587.
[5] Y. Zhang, X. Sun, L. Pan, H. Li, Z. Sun, C. Sun, B.K. Tay, Carbon nanotube–ZnO nanocomposite electrodes for supercapacitors, Solid State Ionics 180 (2009) 1525–1528.
[6] W.-C. Chang, Y.-Y. Cheng, W.-C. Yu, Y.-C. Yao, C.-H. Lee, H.-H. Ko, Enhancing performance of ZnO dye-sensitizedsolar cells by incorporation of multiwall carbon nanotubes, Nanoscale Research Letters 7 (2012) 166. http://www.nanoscalereslett.com/content/7/1/166.
[7] L.S. Aravinda, K.K. Nagaraja, H.S. Nagaraja, K.U. Bhat, B.R. Bhat, ZnO/carbon nanotube nanocomposite for high energy density supercapacitors, Electrochim. Acta 95 (2013) 119–124.
[8] A. Prasannan, T. Imae, One-pot synthesis of fluorescent carbon dots from orange waste peels, Ind. Eng. Chem. Res. 52 (44) (2013) 15673–15678.
[9] B. Devadas, T. Imae, An effect of carbon dots on conducting polymers for energy storage applications, ACS Sustain. Chem. Eng. 6 (2018) 127–134.
[10] M.T. Efa, T. Imae, Hybridization of carbon-dots with ZnO nanoparticles of different sizes, J. Taiwan Inst Chem Eng. 92 (2018) 112–117.
[11] P.-C. Hsu, Z.-Y. Shih, C.-H. Lee, H.-T. Chang, Synthesis and analytical applications of photoluminescent carbon nanodots, Green Chem. 14 (2012) 917–920.
[12] K. Robinson, G.R.A. Kumara, R.J.G.L.R. Kumara, E.N. Jayaweera, R.M.G. Rajapakse, SnO2/ZnO composite dye-sensitized solar cells with graphene-based counter electrodes, Org. Electron. 56 (2018) 159–162.
[13] B. Krishnakumar, T. Imae, J. Miras, J. Esquena, Synthesis and azo dye photodegradation activity of ZrS2–ZnO nano-composites, Separ. Purif. Technol. 132 (2014) 281–288.
[14] M.Y.A. Rahman, A.A. Umar, R. Taslim, M.M. Salleh, Effect of organic dye, the-concentration and dipping time of the organic dye N719on the photovoltaic performance of dye-sensitized ZnO solar cell prepared by ammonia-assisted hydrolysis technique, Electrochim. Acta 88 (2013) 639–643.
[15] W. Kwon, Y.-H. Kim, J.-H. Kim, T. Lee, S. Do, Y. Park, M.S. Jeong, T.-W. Lee, S.-W. Rhee, High color-purity green, orange, and red light-emitting didoes based on chemically functionalized graphene quantum dots, Sci. Rep. 6 (2016) 24205, https://doi.org/10.1038/srep24205(2016).
[16] A. Al-Kahlout, Thermal treatment optimization of ZnO nanoparticles-photoelectrodes for high photovoltaic performance of dye-sensitized solar cells, J Assoc Arab Univ Basic Appl Sci 17 (2015) 66–72.
[17] Y. Yamada, Y. Yamaji, M. Imada, Exciton lifetime paradoxically enhanced by dissipation and decoherence: toward efficient energy conversion of a solar cell, Phys. Rev. Lett. 115 (2015), https://doi.org/10.1103/PhysRevLett.115.197701, 197701-1-6.
[18] D. Cammi, K. Zimmermann, R. Gorny, A. Vogt, F. Dissinger, A. Gad, N. Markiewcz, A. Waag, J.D. Prades, C. Ronning, S.R. Waldvogel, T. Voss, Enhancement of the sub-band-gap photoconductivity in ZnO nanowires through surface functionalization with carbon nanodots, J. Phys. Chem. C 122 (2018) 1852–1859.
[19] Q. Zhang, C.S. Dandeneau, X. Zhou, G. Cao, ZnO nanostructures for dye-sensitized solar cells, Adv. Mater. 21 (2009) 4087–4108.
[20] R. Vittal, K.-C. Ho, Zinc oxide based dye-sensitized solar cells: a review, Renew. Sustain. Energy Rev. 70 (2017) 920–935.
[21] A. Omar, H. Abdullah, S. Shaari, M.R. Taha, Characterization of zinc oxide dye-sensitized solar cell incorporation with single-walled carbon nanotubes, J. Mater. Res. 28 (2013) 1753–1760.
[22] F. Xu, J. Chen, X. Wu, Y. Zhang, Y. Wang, J. Sun, H. Bi, W. Lei, Y. Ni, L. Sun, Graphene scaffolds enhanced photogenerated electron transport inZnO photoanodes for high-efficiency dye-sensitized solar cells, J. Phys. Chem. C 117 (2013) 8619–8627.
[23] C.-H. Hsu, C.-C. Lai, L.-C. Chen, P.-S. Chan, Enhanced performance of dye-sensitized solar cells with graphene/ZnO nanoparticles bilayer structure, J. Nanomater. 2014 (2014). https://doi.org/10.1155/2014/748319.
[24] X. Guo, H. Zhang, H. Sun, M.O. Tade, S. Wang, Green synthesis of carbon quantum dots for sensitized solar cells, ChemPhotoChem 1 (2017) 116–119.
[25] Q. Zhang, G. Zhang, X. Sun, K. Yin, H. Li, Improving the power conversion efficiency of carbon quantum dot-sensitized solar cells by growing the dots on a TiO2 photoanode in situ, Nanomaterials 7 (2017) 130, https://doi.org/10.3390/nano7060130.
[26] A. Kundu, A. Shit, S. Nandi, Carbon dot assisted synthesis of nanostructured polyaniline for dye sensitized solar cells, Energy Fuels 31 (2017) 7364–7371.
[27] W. Zhu, Y. Zhao, J. Duan, Y. Duan, Q. Tang, B. He, Carbon quantum dot tailored counter electrode for 7.01%-rear efficiency in a bifacial dye-sensitized solar cell, Chem. Commun. 53 (2017) 9894–9897.